

## HYDROGENOLYSIS MECHANISMS FOR POLYCYCLIC ALKYLARENES

C. Michael Smith and Phillip E. Savage\*  
University of Michigan, Department of Chemical Engineering  
Ann Arbor, MI 48109-2136

**KEYWORDS:** Alkylpyrenes, Hydrogenolysis, Pyrolysis

### INTRODUCTION

Recent neat pyrolyses of polycyclic alkylaromatics have demonstrated the relatively facile cleavage of strong aryl-alkyl bonds.<sup>1-7</sup> Because these compounds mimic the analogous moieties in coal and oil, their reaction pathways and mechanisms provide insight to reactions occurring in co-processing, coal liquefaction and gasification, and heavy oil upgrading and coking. The hydrogenolysis mechanisms responsible for aryl-alkyl C-C bond cleavage in alkylarenes have not been fully elucidated, but the literature does provide some possibilities.<sup>6-8</sup>

We desired to understand this hydrogenolysis more completely and to employ this understanding to develop a general mechanistic model for alkylarene pyrolysis that was consistent with experimental observations. A general mechanistic reaction model can be developed by conducting experiments with different alkylarenes, taking advantage of results in the literature, and employing the principles embodied in thermochemical kinetics and molecular orbital (M.O.) theory. We have previously reported experimental data (e.g., product molar yields, selectivities, rate constants) for a large number of n-alkylarenes, and we proposed a general pyrolysis network.<sup>3</sup> We also conducted experimental studies using probe molecules to explore different mechanistic scenarios for the hydrogenolysis.<sup>1,2</sup> This paper reports our initial activities aimed at developing a general mechanistic model. We have relied on our experimental results and the literature to provide probable elementary reaction steps, and we used thermochemical kinetics and M.O. theory to estimate their reaction rate constants. Our initial mechanistic models explore the pyrolysis of 1-methyl- and 1-ethylpyrene. Our logic for studying these compounds is twofold. First, the mechanisms responsible for the cleavage of the aryl-alkyl bond in methyl- and ethylpyrene must also be operative during the pyrolysis of alkylarenes with longer chains. Second, the pyrolysis of these compounds leads to a smaller number of products than does the pyrolysis of long-chain alkylarenes. Thus, there is a smaller pool of species from which the hydrogenolysis agents can be chosen, and this reduces the complexity of the mechanistic models. Additionally, for methylpyrene neither  $\alpha$ -alkylpyrene radicals nor aliphatic radicals can participate in the radical hydrogen transfer reactions that others have suggested as potential hydrogenolysis steps<sup>6,8</sup> for long-chain alkylpyrenes. Thus, it is apparent that the simplicity of these pyrolysis systems makes them convenient initial tools for probing different mechanistic scenarios and developing more complex mechanistic models for long-chain alkylarenes.

### EXPERIMENTAL

1-Methylpyrene and 1-ethylpyrene pyrolyses were conducted neat at 400, 425, and 450°C in constant-volume, 316 stainless steel, micro-batch reactors. The reactors were typically loaded with about 10 mg of alkylpyrene and 10 mg of o-terphenyl as an internal standard. After being loaded, the reactors were purged and sealed in a nitrogen-filled glove box and then placed in an isothermal, fluidized sand bath. Upon reaching the desired holding time, the reactors were removed from the fluidized bath, and the reaction was quenched. The products were recovered by repeated extraction with benzene. The reaction products were identified by gas chromatography-mass spectrometry, and their molar yields (i.e., moles of product formed/moles of reactant loaded in reactor) were quantified by capillary column gas chromatography. Details about the experimental protocol have been given previously.<sup>1-4</sup>

### EXPERIMENTAL RESULTS

**1-Methylpyrene:** The pyrolysis of methylpyrene led to pyrene and dimethylpyrene as the major products, and Table I lists the molar yields of these products at different reaction conditions. The minor products included a second dimethylpyrene isomer, ethylpyrene, and four trimethylpyrene isomers. Of these minor products, only the dimethylpyrene isomer was present in yields sufficiently high to quantify. Its molar yield increased steadily at all three

temperatures, and its maximum yield was 1.8% at 150 minutes at 450°C. The recovery of pyrene moieties in the quantified products ranged from nearly 100% to a low of 72% for the reaction at 450°C and 300 minutes. The failure to achieve 100% recovery at the more severe reaction conditions is likely due to the formation of high molecular weight products that did not elute from the GC.

**1-Ethylpyrene:** The pyrolysis of ethylpyrene led to pyrene and methylpyrene as major products, and Table II lists representative results from these experiments. The minor/trace products were diethylpyrene, methylethylpyrene, vinylpyrene, dihydropyrene and a benzene-insoluble char. The molar yield of diethylpyrene typically reached a maximum and then decreased with time. Vinylpyrene and methylethylpyrene were only observed in trace quantities, so their yields were not quantified. The lowest recovery of pyrene units in the quantified products was 72% for the reaction at 450°C and 72 minutes.

#### MECHANISTIC MODELING AND RESULTS

The development of mechanistic models for methyl- and ethylpyrene pyrolysis was guided by experimental observations, by previous mechanistic models for toluene and ethylbenzene pyrolysis, and by previous investigations into the pyrolysis of polycyclic aromatic hydrocarbons. We simulated the pyrolyses using *AcuChem*, a software package developed by the National Institute of Standards and Technology.<sup>9</sup> The program sets up and solves the differential equations that describe species' concentrations as a function of time for reactions in a constant-volume batch reactor.

**1-Methylpyrene:** The 18 elementary step free-radical reaction mechanism used to describe the pyrolysis of methylpyrene is depicted in Figure 1. Methylpyrene undergoes initiation through two possible routes: unimolecular homolytic dissociation and bimolecular reverse radical disproportionation (RRD).<sup>10,11</sup> Chain propagation proceeds via radical hydrogen transfer (RHT),<sup>12</sup> H-atom and methyl radical addition, and methyl radical and H-atom elimination. Finally, termination occurs through the recombination and disproportionation of methylpyrenyl radicals and alkyldihydropyrenyl radicals. This mechanism omits potential secondary reactions such as RRD of dimethylpyrene molecules or RHT to pyrene molecules. Thus, this model will be most valid at low methylpyrene conversions where these secondary reactions are unimportant. The Arrhenius parameters estimated for each step in Figure 1 are listed in Table III, and details of the estimation procedure are given elsewhere.<sup>4</sup>

Figure 2 displays the comparison of the model prediction and experimental observation for the temporal variation of product yields from methylpyrene pyrolysis at 425°C. The model (solid lines) predicts the experimental data (discrete points) well at conversions less than 30%. At higher conversions, however, the model tended to underpredict methylpyrene reactivity. This lack of quantitative agreement at higher conversions could be due to the model's omission of secondary reactions. For example, pyrene could serve as a hydrogen acceptor in RRD reactions, but the model does not include such steps. If it had, the predicted reactivity of methylpyrene would have increased. Overall, however, the agreement between the calculated and the experimental molar yields was reasonably good.

Figure 3 displays the model's prediction of the rates of RRD (reaction 2), RHT (reactions 4 and 5) and H-atom addition (reaction 8), reactions that add hydrogen to the ipso position in methylpyrene, as a function of conversion for the pyrolysis at 425°C. The results at 400 and 450°C were similar to those presented in Figure 3. It is apparent from Figure 3 that the rate of H-atom ipso substitution is typically lower than the rates of RHT and RRD. The rate of RHT by methylhydropyrenyl radicals (step 4) is initially faster than the rate of RRD, but at a conversion of about 0.1 the rate of RRD becomes more significant. The model predicted that this transition point occurred at methylpyrene conversions of about 0.2 and less than 0.1, respectively for pyrolysis at 400°C and 450°C, respectively. Thus, the importance of RHT by methylhydropyrenyl radicals relative to RRD decreases as temperature increases.

The rates of RHT by dimethylhydropyrenyl radicals (step 5) and H-atom substitution (step 8) are lower than those of steps 2 and 4. At 425°C, the rate of RHT by dimethylhydropyrenyl radicals is greater than the rate of H-atom substitution for methylpyrene conversions less than about 0.68. At conversions greater than 0.68, there is a shift in the

importance of these two steps as the rate of step 8 becomes greater than the rate of step 5. This behavior was also observed at the other temperatures studied. For example, at 400 and 450°C, respectively, this transition occurred at methylpyrene conversions of 0.85 and 0.48, respectively. This trend suggests that the importance of step 8 relative to step 5 increases as the temperature increases. This observation that H-atoms become more important as the temperature increases is consistent with previous work.<sup>6,13</sup>

The results of the pyrolysis simulation have revealed that the relative importance of RHT by methylhydropyrenyl radicals decreases and the role of H-atoms increases with increases in temperature. This behavior arises because high temperatures favor  $\beta$ -scission of hydropyrenyl radicals to yield a hydrogen atom rather than direct hydrogen transfer by RHT. This is because the  $\beta$ -scission step has the higher activation energy. Thus, at higher temperatures there is a greater concentration of hydrogen atoms and consequently a higher rate of H-atom ipso substitution.

**1-Ethylpyrene:** The free-radical mechanism for ethylpyrene pyrolysis is shown in Figure 4, and the estimated Arrhenius parameters for each elementary step are summarized in Table IV. Details of their estimation have been discussed elsewhere.<sup>4</sup> As was the case for methylpyrene pyrolysis, initiation in ethylpyrene proceeds through both homolytic dissociation and RRD. The resulting radicals propagate the chain through hydrogen abstraction, RHT, and addition/elimination reactions. Termination proceeds through radical disproportionation.

Figure 5 compares the model predictions and the experimental molar yields of ethylpyrene at 400, 425, and 450°C. Inspection of Figure 5 reveals essentially quantitative accord between the model calculations and the experimentally determined yields of ethylpyrene. Although the model accurately predicted the kinetics of ethylpyrene disappearance, it underpredicted the amount of pyrene and methylpyrene formed, and it overpredicted vinylpyrene formation. For example, at a batch holding time of 150 minutes and at a pyrolysis temperature of 425°C, the predicted molar yields of vinylpyrene, pyrene, and methylpyrene are 0.36, 0.36 and 0.008 respectively. Experimentally, however, vinylpyrene was not observed, and the molar yields of pyrene and methylpyrene were 0.47 and 0.08. One reason for this discrepancy is that the model, which focuses on the primary reactions, does not include the secondary decomposition reactions available for vinylpyrene. Omitted reactions include vinylpyrene polymerization, its reduction to ethylpyrene, and its decomposition to pyrene or methylpyrene. The kinetics and mechanisms of these reactions are not completely resolved and it is for this reason that they were not included in the model. If such steps were included, however, the model would predict a much lower yield of vinylpyrene and increased molar yields of methylpyrene and pyrene as observed experimentally.

Examination of Figure 6, which displays the rates of different elementary reaction steps at 425°C as a function of ethylpyrene conversion, reveals the relative importance of each of the different hydrogen addition mechanisms. Step 15, RHT by ethylhydropyrenyl radicals has the fastest rate of reaction. The next fastest hydrogenolysis step is RRD (step 2) followed by H-atom addition (step 13), RHT by ethyl radicals (step 20), and RHT by  $\alpha$ -ethylpyrene radicals (step 19). The trends that are depicted in Figure 6 were also observed for the simulations at 400 and 450°C. As was observed for the pyrolysis simulation of methylpyrene, RHT by alkylhydropyrenyl radicals and RRD are the major steps that lead to aryl-alkyl bond cleavage. The rates of the other hydrogenolysis steps, however, are not insignificant and can not be ignored. Indeed, the relative importance of H-atoms in ethylpyrene pyrolysis at high conversions stands in contrast to the model results for 1-methylpyrene where H atoms had a less significant contribution to the total hydrogenolysis rate. The increased role of H-atoms in ethylpyrene pyrolysis is likely due to their production through the  $\beta$ -scission of  $\alpha$ -ethylpyrene radicals. To summarize, the results of this simulation suggest that all of the modes of hydrogenolysis included in the simulation can be important in engendering aryl-alkyl bond cleavage in 1-ethylpyrene pyrolysis.

## CONCLUSIONS

1. Hydrogenolysis was the dominant reaction during the neat pyrolysis of methylpyrene. The major pyrolysis products were pyrene and dimethylpyrene. This experimental observation is noteworthy because radical hydrogen transfer by alkyl radicals or by  $\alpha$ -alkylpyrene radicals is not an operable mechanism in this system.

2. The pyrolysis of ethylpyrene led to pyrene and methylpyrene as the major products with pyrene being present in much higher yields. The rate of hydrogenolysis for ethylpyrene was greater than that for methylpyrene.

3. Mechanistic modeling of methylpyrene and ethylpyrene pyrolysis revealed that RRD played an important role in adding hydrogen to the ipso-position and in generating alkylhydropyrenyl radicals that then participated in radical hydrogen transfer steps. In the pyrolysis of methylpyrene, alkylhydropyrenyl radicals generated from methyl radical addition were also hydrogenolysis agents. In ethylpyrene pyrolysis alkylhydropyrenyl radicals were also largely responsible for hydrogenolysis along with contributions from H-atoms, ethyl radicals, and  $\alpha$ -ethylpyrene radicals.

#### ACKNOWLEDGEMENTS

We thank Steven Sherman and Joseph Gullo for performing the methylpyrene pyrolysis experiments. This work was supported in part by the Link Foundation, the Shell Faculty Career Initiation Fund, and the National Science Foundation (CTS-8906859). Acknowledgement is also made to the donors of the Petroleum Research Fund (ACS-PRF # 23744-AC4), administered by the ACS, for the partial support of this research.

#### LITERATURE CITED

1. Smith, C. M.; Savage, P. E. *Ind. Eng. Chem. Res.* **1991**, *30*, 331-339.
2. Smith, C. M.; Savage, P. E. *Energy & Fuels* **1991**, *5*, 146-155.
3. Smith, C. M.; Savage, P. E. *AIChE Journal* **1991**, *37*, 1613-1624.
4. Smith, C. M.; Savage, P. E. *Energy & Fuels* **1992**, *6*, in press.
5. Savage, P. E.; Jacobs, G. E.; Javanmardian, M. *Ind. Eng. Chem. Res.* **1989**, *28*, 645-652.
6. Freund, H.; Maturro, M. G.; Olmsted, W. N.; Reynolds, R. P.; Upton, T. H. *Energy & Fuels*. **1991**, *5*, 840-846.
7. Vlasnik, V. J.; Virk, P. Paper 139D *AIChE Annual Meeting*, Chicago, **1990**.
8. McMillen, D. F.; Malhotra, R.; Tse, D. S. *Energy & Fuels* **1991**, *5*, 179-187.
9. Braun, W.; Herron, J. T.; Kahanen, D. K. *Int. J. Chem. Kinet.* **1988**, *20*, 51-62.
10. Billmers, R.; Brown, R. L.; Stein, S. E. *Int. J. Chem. Kinet.* **1989**, *21*, 375-389.
11. Billmers, R.; Griffith, L. L.; Stein, S. E. *J. Phys. Chem.* **1986**, *90*, 517-523.
12. McMillen, D. F.; Malhotra, R.; Chang, S. J.; Olgier, W. C.; Nigenda, S. E.; Fleming, R. H. *Fuel* **1987**, *66*, 1611-1620.
13. McMillen, D. F.; Malhotra, R.; Nigenda, S. E. *Fuel* **1989**, *68*, 380-386.

**TABLE I: MOLAR YIELDS OF MAJOR PRODUCTS FROM 1-METHYLPYRENE PYROLYSIS**

TEMP (°C)	400	400	400	400	400	400	400
TIME (min)	30	60	90	120	150	240	300
PYRENE	0	0.01	0.01	0.01	0.02	0.05	0.06
DIMETHYLPYRENE	0	0.00	0.01	0.01	0.01	0.03	0.04
METHYLPYRENE	1.01	1.05	0.98	1.03	0.95	0.87	0.85
TEMP (°C)	425	425	425	425	425	425	425
TIME (min)	30	60	90	120	165	240	300
PYRENE	0.01	0.05	0.07	0.1	0.15	0.22	0.22
DIMETHYLPYRENE	0	0.04	0.04	0.06	0.09	0.12	0.11
METHYLPYRENE	0.97	0.90	0.90	0.83	0.67	0.57	0.54
TEMP (°C)	450	450	450	450	450	450	450
TIME (min)	30	60	90	120	150	240	300
PYRENE	0.06	0.15	0.22	0.26	0.31	0.39	0.37
DIMETHYLPYRENE	0.03	0.08	0.10	0.10	0.09	0.01	0.01
METHYLPYRENE	0.88	0.66	0.50	0.42	0.41	0.35	0.35

**TABLE II: MOLAR YIELDS OF MAJOR PRODUCTS FROM 1-ETHYLPYRENE PYROLYSIS**

TEMP (°C)	400	400	400	400	400	400	400
TIME (min)	45	70	90	110	150	200	320
PYRENE	0.20	0.47	0.13	0.37	0.44	0.61	0.60
METHYLPYRENE	0.02	0.05	0.01	0.04	0.05	0.11	0.11
ETHYLPYRENE	0.91	0.80	0.82	0.52	0.47	0.41	0.26
TEMP (°C)	425	425	425	425	425	425	425
TIME (min)	65	80	115	135	150	180	205
PYRENE	0.52	0.49	0.54	0.64	0.47	0.61	0.62
METHYLPYRENE	0.07	0.08	0.10	0.11	0.09	0.07	0.13
ETHYLPYRENE	0.55	0.41	0.32	0.33	0.18	0.13	0.17
TEMP (°C)	450	450	450	450	450	450	450
TIME (min)	20	30	42	50	60	72	80
PYRENE	0.45	0.48	0.56	0.47	0.68	0.48	0.74
METHYLPYRENE	0.08	0.08	0.10	0.10	0.14	0.11	0.13
ETHYLPYRENE	0.58	0.46	0.25	0.19	0.17	0.13	0.13

TABLE III: ARRHENIUS PARAMETERS FOR 1-METHYLPYRENE PYROLYSIS

Reaction Number in Figure 1	$\log_{10} A$ ( $s^{-1}$ or Liter mole $^{-1} s^{-1}$ )	Activation Energy (kcal mole $^{-1}$ )	Reaction Path Degeneracy
1	16	82.9	3
2	8	45.8	6
3	8	45.8	18
-3	9.5	0	-
4	8.1	16.5	2
5	8.1	16.5	1
6	8.1	16.5	3
7	10.4	2.3	3
8	10.4	2.3	1
9	8.8	4.1	3
-9	13.9	29.4	1
10	13.9	35.3	2
11	13.9	29.4	1
12	11.1	5.6	3
13	8.5	6.9	3
14	9.5	0	-
-14	16	51.2	1
15	9.5	0	-

TABLE IV: ARRHENIUS PARAMETERS FOR 1-ETHYLPYRENE PYROLYSIS

Reaction Number in Figure 4	$\log_{10} A$ ( $s^{-1}$ or Liter mole $^{-1} s^{-1}$ )	Activation Energy (kcal mole $^{-1}$ )	Reaction Path Degeneracy
1	16	69.6	1
2	8	42.8	4
3	8	42.8	12
4	14.0	53.6	3
5	13.9	35.3	2
6	14	20	1
7	12.9	38.4	3
8	11.1	5.6	2
9	8.5	5.4	2
10	8.5	8.9	2
11	8.8	15.5	2
12	10.3	2.3	3
13	10.3	2.3	1
14	9	6	3
15	8.1	16.5	2
16	8.1	16.5	1
17	8.1	16.5	3
18	8.1	25	9
19	8.1	25	3
20	8.4	14.5	3
21	8.4	14.5	9
22	9.5	0	-
23	9.5	0	-

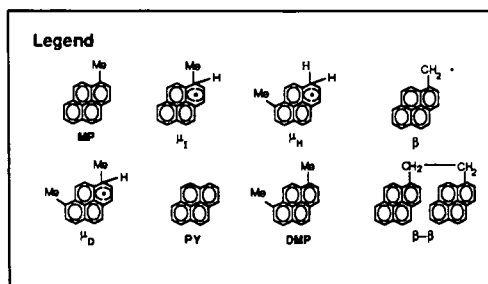
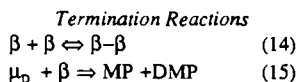
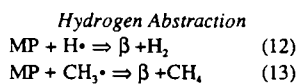
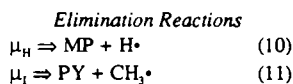
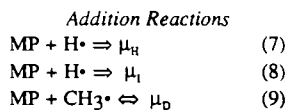
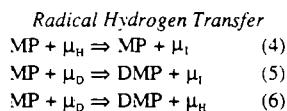
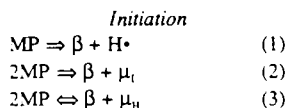


Figure 1: 1-Methylpyrene Pyrolysis Mechanism

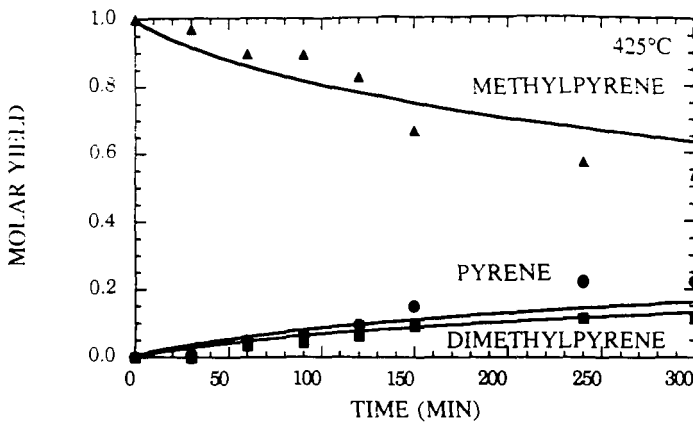


Figure 2: Model and Experimental Results for 1-Methylpyrene Pyrolysis at 425°C

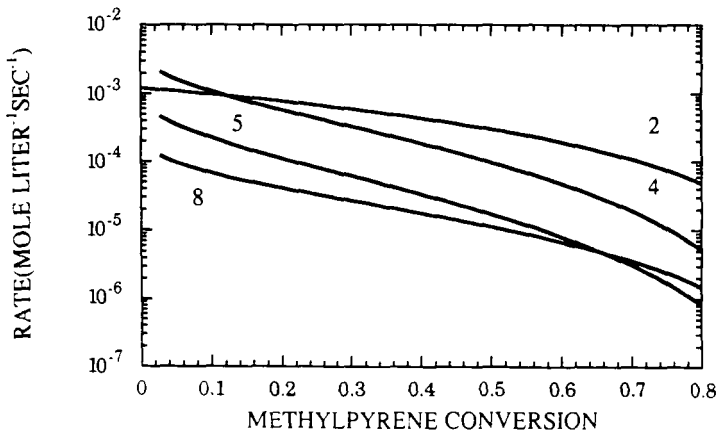


Figure 3: Hydrogenolysis Rates Calculated for 1-Methylpyrene Pyrolysis at 425°C (step 2 is RRD, steps 4 and 5 are RHT, step 8 is H atom addition)

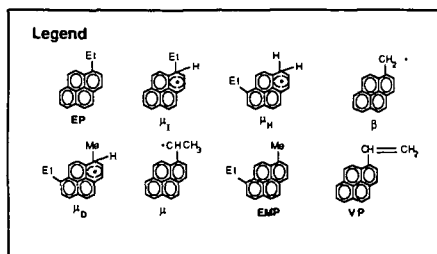
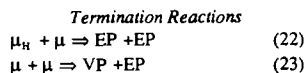
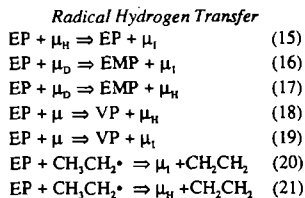
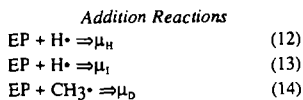
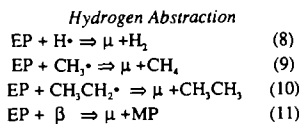
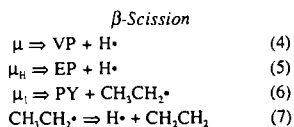
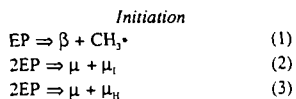


Figure 4: 1-Ethylpyrene Pyrolysis Mechanism

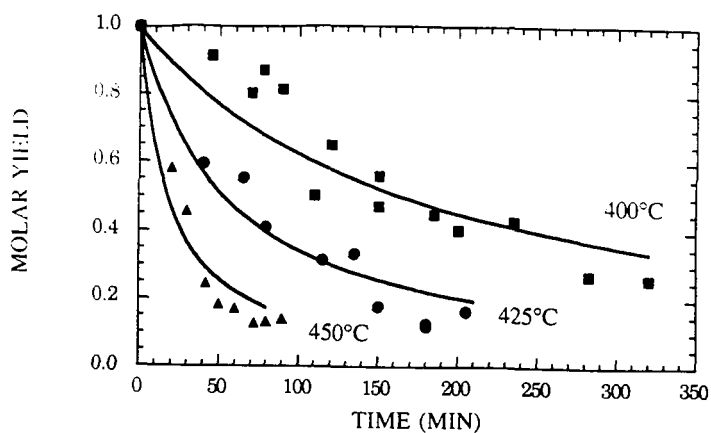


Figure 5: Model and Experimental Results for 1-Ethylpyrene Pyrolysis Kinetics

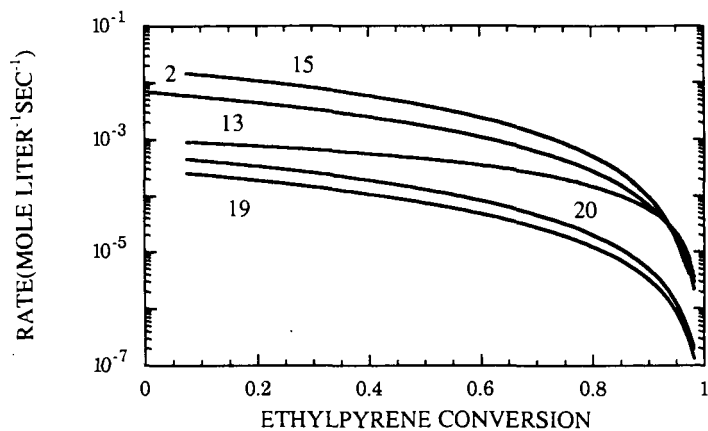


Figure 6: Hydrogenolysis Rates Calculated for 1-Ethylpyrene Pyrolysis at 425°C (step 2 is RRD, step 15 is RHT by ethylhydropyrenyl radicals, step 13 is H atom addition, step 20 is RHT by ethyl radicals, and step 19 is RHT by  $\alpha$ -ethylpyrene radicals)